Article

In-House Standard Method for Molecular Characterization of Dissolved Organic Matter by FT-ICR Mass Spectrometry

Chen He, Yahe Zhang, Yunyun Li, Xiaocun Zhuo, Yuguo Li, Chuanlun Zhang, and Quan Shi*

Cite This: *ACS Omega* 2020, 5, 11730−11736

Read Online

ACCESS | Metrics & More | Article Recommendations | SI Supporting Information

ABSTRACT: Electrospray ionization (ESI) coupled with Fourier transform ion cyclotron resonance mass spectrometry (FT-ICR MS) has been widely used for molecular characterization of dissolved organic matter (DOM). However, ESI FT-ICR MS generally has poor repeatability and reproducibility because of its inherent ionization mechanism and structural characteristics, which severely hindered its application in quantitative analysis of complex mixtures. In this article, we developed an in-house standard method for molecular characterization of DOM by ESI FT-ICR MS. Instead of obtaining reproducible results by determining the instrument parameters, we adopted an approach of object control on the mass spectrum to solve the problem of poor reproducibility. The mass peak shape, resolution, and relative intensity distribution of a natural organic matter standard were adjusted by optimizing the operating conditions to obtain a repeatable result. The quality control sample was run 26 times by the different operators in a 6-month-long period to evaluate the reproducibility. Results showed that the relative standard deviation (%) of repeatability and reproducibility are 1.02 and 2.35 for average H/C, respectively. The in-house standard method has been validated and successfully used for the characterization of more than 4000 DOM samples, which is transferable to other laboratories.
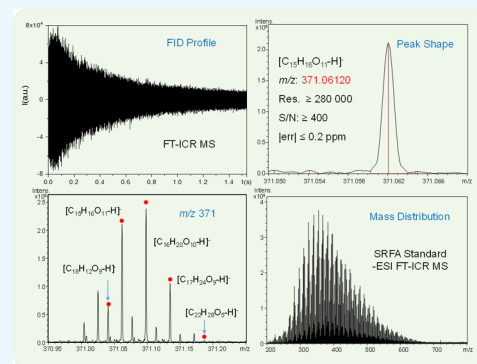
■ INTRODUCTION

Dissolved organic matter (DOM) is a major chemical component involved in the physical, chemical, and biological processes of many aquatic ecosystems[1,2] and constitutes the main organic contaminant in various wastewaters.[3] Therefore, the characterization of the structure and functions of DOM has been a topic of growing interest in environmental science and engineering, biogeochemistry, and other research communities. DOM is one of the most complex naturally occurring mixtures,[4] which has the following features:[5−10] (i) the relative molecular weight of most molecules is less than 1000 Da, which is small compared with bio-macromolecules; (ii) the molecular composition is very complex, making it impossible to characterize the individual compounds by separation techniques such as chromatography; and (iii) high-resolution mass spectrometry is the only effective approach for analyzing the molecular composition; however, the requirement for the resolving power of mass spectrometry is ultrahigh.[11]

Fourier transform ion cyclotron resonance mass spectrometry (FT-ICR MS) with high resolving power and mass accuracy has become a powerful tool to study the molecular composition of small-molecule organic complex mixtures such as petroleum[12] and DOM samples.[13] Electrospray ionization (ESI) can selectively ionize polar compounds, making it an ideal ion source for DOM analysis.[14] Therefore, ESI FT-ICR MS has been successfully applied in the compositional analysis of DOM from different sources, including various surface and underground waters,[15,16] domestic sewages,[17] industrial waste-

waters,[18] soils,[19] sediments,[20] and atmospheric aerosols.[21] In the past two decades, the utilization of ESI FT-ICR MS for the analysis of DOM samples has been increasing dramatically; for example, the publication has increased by nearly 300% from 2010 to 2020 (Figure 1).

Fiever et al.[22] reported the first application of ESI FT-ICR MS for the molecular characterization of humic and fulvic acids from the Suwannee River. In 2003, Kim et al.[23] proposed an approach involving the use of C_{18} solid-phase extraction (SPE) coupled with ESI FT-ICR MS for obtaining the molecular composition of DOM from river water. Nowadays, SPE is mostly used for desalting and concentrating DOM before ionization.[24] The van Krevelen (VK) diagram is commonly used for visualizing the FT-ICR MS data, by plotting molecular H/C vs O/C ratios in a two-dimension diagram.[23] Each molecular formula aligned on the VK diagram can be correlated to commonly associated natural biomolecules. Compounds in different regions of the VK diagram are lipids, proteins, amino sugars, carbohydrates, unsaturated hydrocarbons, condensed aromatics, lignin, and tannins.[25,26] It is
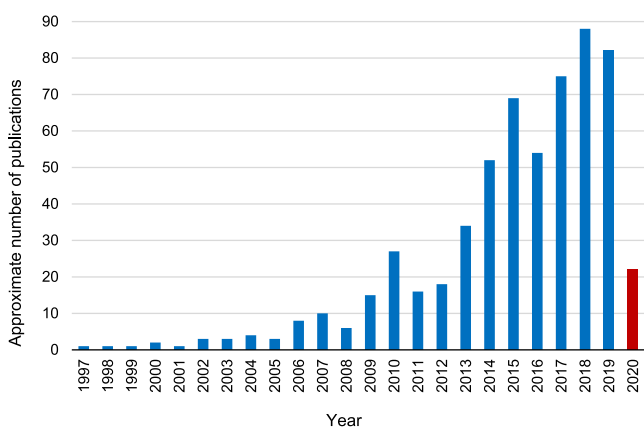
Figure 1. Publications relevant to the topic of dissolved organic matter (water, sediment, soil, aerosol, etc.) analyzed using FT-ICR MS (summarized in February, 2020).

worth noting that these compound classes are not strictly representative of all similar molecules but merely approximate criteria for identifying similarly composed compounds. In addition, the classification of compounds based on the O/C and H/C ratios is not exact for samples with different origins.[27]

In 2006, the aromatic index (AI) was proposed by Koch and Dittmar,[28] which can be calculated by the molecular formulae assigned from the FT-ICR mass spectra. With the combination of AI, H/C, and O/C, DOM can be assigned to the following groups:[29] polycyclic aromatics, highly aromatic compounds, highly unsaturated compounds, unsaturated aliphatic compounds containing N, unsaturated aliphatic compounds, and saturated compounds. The bioavailability of these compounds increases, while the degree of refractory degradation decreases successively.[30,31] The molecular lability index (MLB)[32] was developed by D'Andrilli to estimate the overall lability of DOM: higher MLB indicates high lability. Medeiros et al.[33] used FT-ICR MS to identify 184 molecular formulae that are indicators of riverine inputs. Refractory "carboxyl-rich alicyclic molecules"[34] and "island of stability" compounds[35,36] were characterized in marine DOM using FT-ICR MS combined with nuclear magnetic resonance spectrometry and $\Delta^{14}C$ values, respectively.

Collision-induced dissociation investigation showed that the major functional groups in DOM are carboxyl and hydroxyl[37] and there are at least a 100 thousand different compounds in DOM each present in seawater at picomolar concentrations.[38] Molecular composition reflects the DOM origin and its transformation with chemical or biochemical degradation, which implicate valuable information in geochemistry and microbiology. For these purposes, multivariate statistical methods, such as hierarchal cluster analysis,[39,40] nonmetric multidimensional scaling,[41−43] indicator species analysis,[40] and principal component analysis,[44−47] were combined with visualization diagrams to evaluate the relationships among sample sets. Statistical analysis has become widely used for various studies; however, fewer researchers noted that their data obtained from FT-ICR MS analysis could be unreliable for statistical analysis because both the repeatability and reproducibility of the ESI FT-ICR MS analysis are very poor without a standard method for quality control.

The reproducibility of analytical results is critical in the application of the molecular composition provided by mass spectrometry, which was used to study source apportionment

of DOM, as well as its environmental or geochemical implications. However, the ESI FT-ICR MS mass spectra of standard DOM samples were different and even had a wide discrepancy from different research groups.[7,37,48] For example, there were normal and bimodal distributions of mass spectra for Suwannee River fulvic acids (SRFAs) and the normal distribution of mass spectra had different peak centers. These indicate that FT-ICR MS has poor reproducibility and the data from different labs are incomparable. The main reasons for these differences are as follows: (1) ESI is a competitive ionization source and is susceptible to matrixes such as solvents and impurities;[49] (2) ions need to be multistep focused and accelerated to enter the ion cyclotron resonance (ICR) cell, and high ion transport efficiency can only be achieved by optimizing the ion optics and transmission parameters;[50] (3) the real-time vacuum of the ICR cell has a great effect on the ion detection;[51] and (4) there are structural differences between different models of FT-ICR MS.[52]

Kido Soule et al.[53] have investigated the impact of instrument and experiment parameters on the reproducibility of ESI FT-ICR mass spectra for natural organic matter (NOM). However, the authors focused on peak detection and provided little discussion on the relative peak intensity reproducibility. Sleighter et al.[54] established a standard level of reliability for relative peak intensities of ESI FT-ICR mass spectra for NOM. The reproducibility of peak intensities at each nominal mass was evaluated; however, the relative abundance of mass peaks in a large range was not mentioned. Meanwhile, the samples were tested with triplicate injections on the same day but not on different days. On the whole, reproducibility is a critical issue so far for the molecular composition analysis of DOM.

In this article, we introduce an in-house standard method for the molecular characterization of DOM by FT-ICR MS.

■ RESULTS AND DISCUSSION

Method Development. FT-ICR MS has a long ion transformation pathway to introduce the ions from the atmospheric pressure ESI ionization source to the high-vacuum ion cyclotron cell. The mass spectrum is affected by the ionization, ion transmission, and detection processes; therefore, any operation parameter has a sensitive effect on the shape and quality of the mass spectrum. The effect of each parameter is provided in the Supporting Information.

Theoretically, to obtain repeating spectra, it needs to be ensured that ionization, ion transmission, and ion detection processes of each test are consistent, which in fact, is hard to be carried out on the most recently available FT-ICR MS. For example, because of the continuous contamination of electrodes in the instruments, both the ionization and transfer efficiencies cannot be stabilized at a consistent value; in other words, the spectra will be different even if the instrument parameters do not change.

The principle of our proposed method is to take the mass spectral shape and quality of a standard sample as the control target to make repeatable and comparable results. The mass peak shape, resolution, and relative intensity distribution of a natural organic matter standard were adjusted by optimizing the operating conditions. A schematic flow is shown in Figure 2. The international standard substance, SRFA, was selected as the quality control sample. SRFA was dissolved in methanol at a concentration of 100 mg/L and ultrasound for 10 min before FT-ICR MS analysis. The shape and quality of the optimized
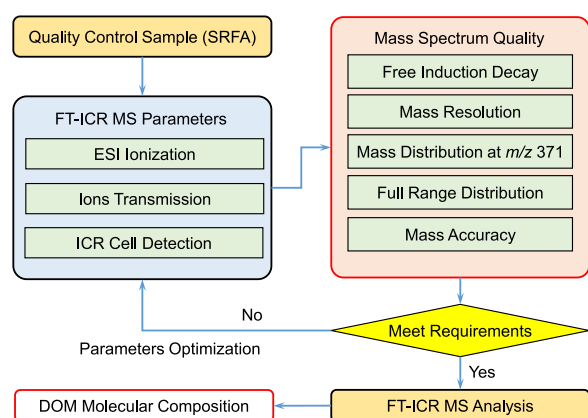
Figure 2. Schematic flow of the proposed standard method.

mass spectrum include the following aspects: (1) free induction decay, (2) mass resolution, (3) relative peak intensity (at m/z 371 and overall mass spectrum), and (4) mass accuracy. The optimization was performed step by step and could go through several cycles if needed. Only when all of the requirements of these aspects are well met, the instrument can be used for real sample analysis.

Free Induction Decay (FID). FT-ICR MS acquires the time-domain frequency signal generated in the ICR cell induced by the ion resonance. The FID is generally observed with a cone-like profile. To obtain a high resolution, a long transient length is needed. However, if the ions quench in a shorter time than the acquisition time, noise will be calculated in the Fourier

transform processing and lead to a pseudo-high-resolution mass spectrum. In addition, the profile of the spectrum will vary randomly and the mass spectral peak is asymmetrical. Unfortunately, it is hard to maintain a long transient time, especially for the old model commercial FT-ICR MS instruments. Therefore, to strike a balance between the high resolution and high "signal quality" is critical for instrument optimization. A good-quality FID signal should last for the duration of the collision period, that is, the signal intensity continually decays with time, forming a cone-like profile. In this proposed method, we require that the FID signal keep a continuous decay within the full transient time (Figure 3a). Under this premise, other ICR cell parameters and Fourier transform parameters, such as the window function and zero fill times, were optimized or selected to obtain symmetrical normal distribution peaks both in the lower and the higher ends of the mass spectrum.

Mass Resolution. It is well known that a high resolution is necessary for the molecular characterization of DOM; however, as mentioned above, high-quality mass peak is more important for repeatability and reproducibility. We selected m/z 371.0620 (corresponding to $[C_{15}H_{16}O_{11}-H]^-$), which was in the center of the mass range and close to the most abundant peak in the mass spectrum, as the reference peak. The resolution power of this peak was required to be not less than 280 000 (Figure 3b). This is not a high value in resolution for FT-ICR MS, however, it generally meets the requirement of the analysis. In addition, we lower the requirement of resolution to make it comparable with the
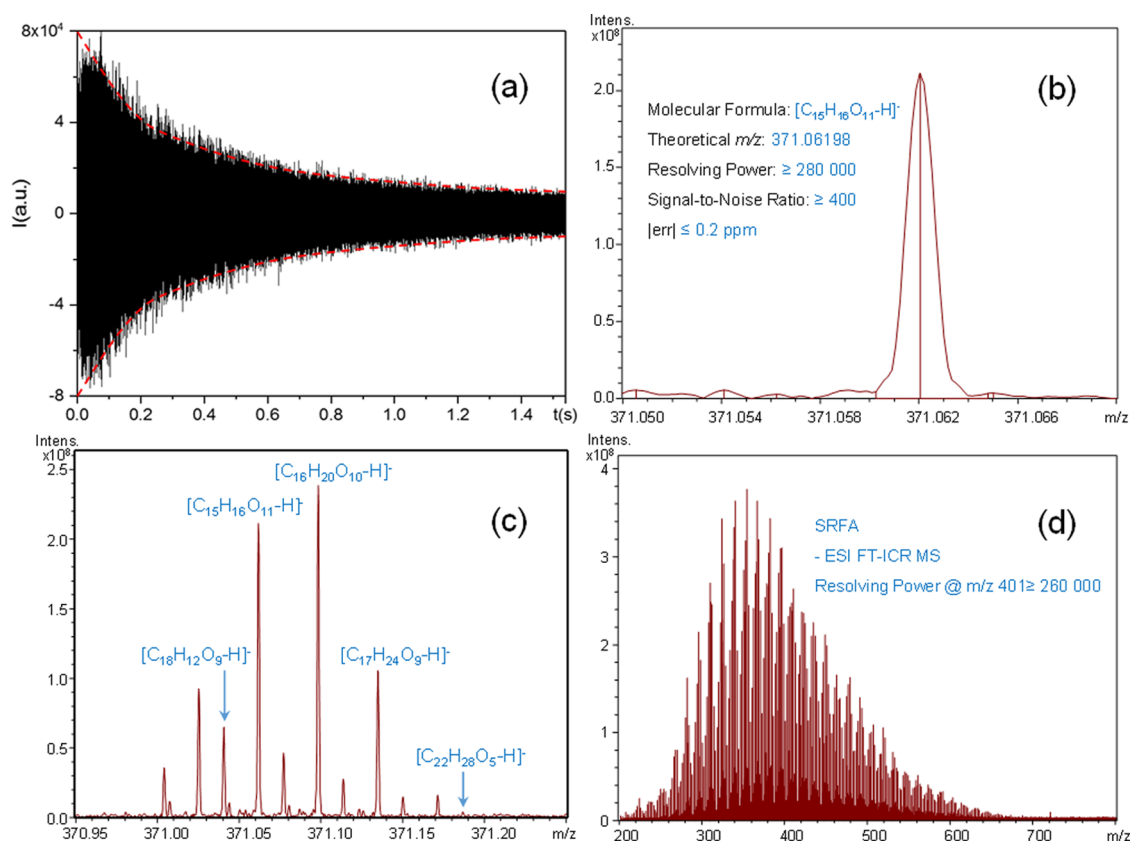
Figure 3. Suwannee River fulvic acid (SRFA) analyzed by negative-ion ESI FT-ICR MS: (a) time-domain free induction decay (FID), (b) mass scale-expanded segment at m/z 371.05−371.07, (c) mass scale-expanded segment at m/z 370.95−371.25, and (d) broadband mass spectrum.

results from our Orbitrap MS. In other words, the standard method is transplantable between different MS platforms.

Relative Peak Intensity. Consistent relative peak intensity is the most important objective for instrument optimization. We selected two sets of mass peaks to evaluate the relative abundance distribution.

Isobaric Peaks at m/z 371. The relative peak intensity within a nominal mass usually has good reproducibility. Sleighter et al.[54] reported that the average percentage relative standard deviation (RSD, standard deviation divided by the relative peak intensity) at the signal-to-noise ratio (S/N) 5 was 8%. Here, four peaks at m/z 371 were used to evaluate the spectrum. As shown in Figure 3c, the base peak at m/z 371 is the quasi-molecular ion peak of $[C_{16}H_{20}O_{10}-H]^-$. The relative peak intensity ranges between the base peak and three other peaks of $[C_{18}H_{12}O_9-H]^-$, $[C_{15}H_{16}O_{11}-H]^-$, and $[C_{17}H_{24}O_9-H]^-$ were restricted at 23 ± 8, 83 ± 10, and 54 ± 10% (shown in Table 1), respectively. At the same time, we restrict the

Table 1. Quantitative Constraints on Relative Peak Intensity at m/z 371

theoretical m/z	molecular formula	relative intensity (%)	S/N
371.0409	$[C_{18}H_{12}O_9-H]^-$	23 ± 8	≥120
371.0620	$[C_{15}H_{16}O_{11}-H]^-$	85 ± 10	≥400
371.0984	$[C_{16}H_{20}O_{10}-H]^-$	100	≥550
371.1348	$[C_{17}H_{24}O_9-H]^-$	54 ± 10	≥200

minimum S/N value of these four peaks (Table 1). In addition, the S/N value of the quasi-molecular ion peak of $[C_{22}H_{28}O_5-H]^-$ should not be less than 6.

Relative Peak Intensity of the Overall Mass Spectrum. Comparing with that at m/z 371, the relative peak intensity of the overall mass spectrum has greater effects on the FT-ICR MS result and is more sensitive to instrument conditions. The mass range of SRFA is between 200 and 700 Da with a center of the normal distribution at around m/z 355 (Figure 3d). Seven peaks were selected to quantify the ratio of the peak intensity of the overall mass spectrum. These seven peaks were 251.0197, 311.0772, 355.1034, 411.0932, 463.0517, 519.0418, and 573.0524, corresponding to ions of $[C_{11}H_8O_7-H]^-$, $[C_{14}H_{16}O_8-H]^-$, $[C_{16}H_{20}O_9-H]^-$, $[C_{18}H_{20}O_{11}-H]^-$, $[C_{20}H_{16}O_{13}-H]^-$, $[C_{22}H_{16}O_{15}-H]^-$, and $[C_{25}H_{18}O_{16}-H]^-$, respectively. The seven selected peaks cover most of the mass range. The relative peak intensities and minimum S/N values of these seven peaks are shown in Table 2. In addition, the S/N value of the quasi-molecular ion peak of $[C_9H_6O_7-H]^-$ (theoretical m/z 225.0041) and $[C_{27}H_{20}O_{18}-H]^-$ (theoretical m/z 631.0576) should be not less than 10.

Mass Accuracy. High mass accuracy is essential for molecular assignment and always expected for mass spectro-

Table 2. Quantitative Constraints on Relative Peak Intensities of Reference Peaks in a Large Mass Range

theoretical m/z	molecular formula	relative intensity (%)	S/N
251.0197	$[C_{11}H_8O_7-H]^-$	8 ± 5	≥60
311.0772	$[C_{14}H_{16}O_8-H]^-$	55 ± 15	≥500
355.1034	$[C_{16}H_{20}O_9-H]^-$	95 ± 5	≥800
411.0932	$[C_{18}H_{20}O_{11}-H]^-$	70 ± 10	≥500
463.0517	$[C_{20}H_{16}O_{13}-H]^-$	50 ± 15	≥300
519.0418	$[C_{22}H_{16}O_{15}-H]^-$	25 ± 15	≥120
573.0524	$[C_{25}H_{18}O_{16}-H]^-$	12 ± 8	≥80

metric analysis; however, this is not an important criterion for this method. We required that the mass accuracy of the seven peaks mentioned above (Relative Peak Intensity of the Overall Mass Spectrum) be within 0.5 ppm.

Method Evaluation. *Repeatability and Reproducibility of the Relative Peak Intensity.* The quality control sample (SRFA) was analyzed three times by the same operator at one time. Repeatability and reproducibility of relative peak intensity at m/z 371 and other reference mass peaks are listed in Tables 3 and 4, respectively. The repeatability RSD of

Table 3. Repeatability and Reproducibility of Relative Peak Intensity at m/z 371

	repeatability			reproducibility		
theoretical m/z	average relative intensity (%)	SD (%)	RSD (%)	average relative intensity (%)	SD (%)	RSD (%)
371.0409	20.49	0.17	0.84	25.15	3.89	15.45
371.0620	80.02	4.15	5.18	83.82	6.17	7.36
371.0984	100	0	0	100.00	0.00	0.00
371.1348	52.61	0.48	0.91	51.58	5.23	10.14

Table 4. Repeatability and Reproducibility of Relative Intensity of Overall Mass Peaks

	repeatability			reproducibility		
theoretical m/z	average relative intensity (%)	SD (%)	RSD (%)	average relative intensity (%)	SD (%)	RSD (%)
251.0197	7.56	1.50	19.78	8.50	2.42	28.43
311.0772	58.68	1.03	1.75	60.32	6.68	11.07
355.10340	93.77	1.40	1.49	92.36	4.92	5.33
411.0932	68.46	1.30	1.89	68.83	4.55	6.60
463.0517	42.16	0.59	1.41	45.65	6.50	14.24
519.042	23.32	0.53	2.27	24.40	5.77	23.65
573.0524	11.38	0.87	7.67	11.86	3.92	33.03

relative peak intensity from the three analyses was less than 10% except for the peak at theoretical m/z 251.0197. The reproducibility was evaluated by results from the analysis carried out 26 times by different operators at different days in a period of 6 months. The reproducibility RSD of the relative peak intensity at m/z 371 is shown in Table 3. The tallest peak at m/z 371 is the same in all replicate analyses. The reproducibility RSDs of the rest of relative peak intensities at m/z 371 are 15.45, 7.36, and 10.14% for A, B, and C, respectively. For the overall mass peak, the reproducibility RSD is higher at the high and low mass ends and smaller as it is closer to the mass center. Overall, the reproducibility RSD ranges from 5.33 to 33.03% for the evaluated peaks, as shown in Table 4.

Repeatability and Reproducibility of Average Molecular Parameters. Molecular formulae of SRFA were assigned to the detected mass peaks with S/N ratio at least >6. Various intensity-weighted parameters were calculated, including the number of the formulae (no.), m/z_{wa}, C_{wa}, H_{wa}, O_{wa}, N_{wa}, S_{wa}, O/C_{wa}, H/C_{wa}, DBE_{wa}, and $AI_{mod,wa}$. Except S_{wa}, the repeatability and reproducibility RSD of these average molecular parameters are less than 3 and 10%, respectively. The high RSD for S_{wa} is due to the low value (only 0.02) of itself (Table 5).

Table 5. Repeatability and Reproducibility of FT-ICR MS Intensity-Weighted Average (wa) Molecular Parameters of SRFA[a]

	repeatability			reproducibility		
	average value	SD (%)	RSD (%)	average value	SD (%)	RSD (%)
no.	3334	93.39	2.8	3189	285.51	8.95
m/z_{wa}	415.68	3.85	0.92	414.48	10.13	2.44
C_{wa}	18.83	0.256	1.36	18.80	0.54	2.87
H_{wa}	18.13	0.45	2.49	17.90	0.82	4.60
O_{wa}	10.62	0.04	0.33	10.59	0.24	2.22
N_{wa}	0.05	0.001	2.73	0.06	0.004	6.35
S_{wa}	0.02	0.007	28.88	0.02	0.01	38.68
O/C_{wa}	0.57	0.01	1.04	0.57	0.01	1.82
H/C_{wa}	1.02	0.01	1.02	1.01	0.02	2.35
DBE_{wa}	10.3	0.03	0.32	10.38	0.29	2.79
$AI_{mod,wa}$	0.37	0.01	1.54	0.37	0.01	3.64

[a]No.: number of assigned formulae; O/C: oxygen to carbon ratio; H/C: hydrogen to carbon ratio; DBE: double bond equivalents; AI_{mod}: modified aromaticity index.

CONCLUSIONS

Based on the quantitative constraints of mass resolution, mass accuracy, and the relative intensity of the mass spectrum, a standard for molecular characterization of DOM negative-ion ESI FT-ICR MS was developed. Based on the evaluation of relative peak intensity and average molecular parameters, it is confirmed that the method has good repeatability and reproducibility, which is shown by the average H/C of 1.02 and 2.3S, respectively. The standard has been used for the successful characterization of more than 4000 samples and has potential for application in other laboratories. Further work should consider establishing a versatility standard based on the different types of instruments.

EXPERIMENTAL SECTION

Samples and Chemicals. The SRFA sample (2S101F) was purchased from the International Humic Substances Society (IHSS). Methanol was of analytical grade and further distilled for use during all experiments.

ESI FT-ICR MS Analysis. The MS analysis of SRFA was carried out on a 9.4 T Bruker Apex-Ultra FT-ICR mass spectrometer coupled with a negative-ion Apollo II ESI. The SRFA samples were dissolved in methanol at the concentration of 100 mg/L and were injected into the ionization source through a syringe pump. The key operating parameters of FT-ICR MS are presented in Table S1 (see Supporting Information). The mass range was set at m/z 200−800. The data size was set to 2 M words. A total of 128 continuous scans were co-added on each analysis to enhance the signal-to-noise ratio (S/N) of the mass spectrum.

The SRFA samples were analyzed three times on the same day and 26 times within 6 months to evaluate repeatability and reproducibility. In the first 20 days, the samples were tested every 3−4 days, and 2−3 data were collected on 1 day; a total of 21 data were collected. For the next 5 months, one data was collected each month.

Mass Calibration and Molecular Formula Assignments. The mass spectrometer was initially calibrated using sodium formate and then recalibrated with a known mass series in SRFA, which contains a relatively high abundance of CHO formulae, providing a mass accuracy of 0.2 ppm or

higher throughout the mass range of interest. The mass peaks with S/N greater than 6 ranging from 200−800 m/z unit and their peak intensity were exported to a spreadsheet. Data analysis was performed using in-house software. A molecular formula calculator generated matching formulae according to elemental combinations of $^{12}C_{1-60}$, $^{1}H_{1-120}$, $^{14}N_{0-3}$, $^{16}O_{0-30}$, and $^{32}S_{0-1}$. The mass accuracy window was set to 1.0 ppm in the formula assignment section. All elemental formulae should meet basic chemical criteria:[55] (1) the number of H atoms should be at least 1/3 that of C atoms and cannot be greater than that of 2C + N + 2; (2) the sum number of N and H atoms should be even; and (3) the H/C and O/C value should be restricted to be less than 3 and 1.5, respectively.

FT-ICR MS Data Related Parameter Integration. A modified aromatic index (AI_{mod}) and double bond equivalent (DBE) were calculated for each assigned formula according to Koch and Dittmar.[28] The intensity-weighted average of elements (C, H, O, N, S) and other parameters (m/z, H/C, O/C, DBE, and AI_{mod}) were calculated for each analysis.

ASSOCIATED CONTENT

Supporting Information

The Supporting Information is available free of charge at https://pubs.acs.org/doi/10.1021/acsomega.0c01055.

> Key operating parameters of the Apex-Ultra FT-ICR MS, including ionization, ion transformation, and mass analysis; key operating parameters of the instrument and the document of the method HOP 002-2019: Standard test method for molecular characterization of dissolved organic matter by negative-ion ESI FT-ICR MS (PDF)

AUTHOR INFORMATION

Corresponding Author

Quan Shi − State Key Laboratory of Heavy Oil Processing, Petroleum Molecular Engineering Center (PMEC), China University of Petroleum, Beijing 102249, China; orcid.org/0000-0002-1363-1237; Phone: +86 10 89739157; Email: sq@cup.edu.cn

Authors

Chen He − State Key Laboratory of Heavy Oil Processing, Petroleum Molecular Engineering Center (PMEC), China University of Petroleum, Beijing 102249, China

Yahe Zhang − State Key Laboratory of Heavy Oil Processing, Petroleum Molecular Engineering Center (PMEC), China University of Petroleum, Beijing 102249, China

Yunyun Li − State Key Laboratory of Heavy Oil Processing, Petroleum Molecular Engineering Center (PMEC), China University of Petroleum, Beijing 102249, China

Xiaocun Zhuo − State Key Laboratory of Heavy Oil Processing, Petroleum Molecular Engineering Center (PMEC), China University of Petroleum, Beijing 102249, China

Yuguo Li − State Key Laboratory of Heavy Oil Processing, Petroleum Molecular Engineering Center (PMEC), China University of Petroleum, Beijing 102249, China

Chuanlun Zhang − State Key Laboratory of Heavy Oil Processing, Petroleum Molecular Engineering Center (PMEC), China University of Petroleum, Beijing 102249, China; Shenzhen Key Laboratory of Marine Archaea Geo-Omics, Department of Ocean Science & Engineering, Southern University of Science and Technology, Shenzhen 518055, China

Complete contact information is available at:

https://pubs.acs.org/10.1021/acsomega.0c01055

Author Contributions

C.H. and Y.Z. contributed equally to this work; they organized and implemented the experiment; wrote the manuscript and the standard method document. Y.L., X.Z., and Y.L. carried out a part of the experiment and evaluated the method. C.Z. organized the project and revised the manuscript. Q.S. designed and guided the entire project and corrected the manuscript.

Notes

The authors declare no competing financial interest.

■ REFERENCES

(1) Moran, M. A.; Zepp, R. G. Role of Photoreactions in the Formation of Biologically Labile Compounds from Dissolved Organic Matter. *Limnol. Oceanogr.* **1997**, *42*, 1307−1316.

(2) Wu, F.; Tanoue, E. Isolation and Partial Characterization of Dissolved Copper-Complexing Ligands in Streamwaters. *Environ. Sci. Technol.* **2001**, *35*, 3646−3652.

(3) Yuan, Z.; He, C.; Shi, Q.; Xu, C.; Li, Z.; Wang, C.; Zhao, H.; Ni, J. Molecular Insights into the Transformation of Dissolved Organic Matter in Landfill Leachate Concentrate during Biodegradation and Coagulation Processes Using ESI FT-ICR MS. *Environ. Sci. Technol.* **2017**, *51*, 8110−8118.

(4) Kim, S.; Kaplan, L. A.; Hatcher, P. G. Biodegradable dissolved organic matter in a temperate and a tropical stream determined from ultra-high resolution mass spectrometry. *Limnol. Oceanogr.* **2006**, *51*, 1054−1063.

(5) Leenheer, J. A.; Rostad, C. E.; Gates, P. M.; Furlong, E. T.; Ferrer, I. Molecular resolution and fragmentation of fulvic acid by electrospray ionization/multistage tandem mass spectrometry. *Anal. Chem.* **2001**, *73*, 1461−1471.

(6) D'Andrilli, J.; Foreman, C. M.; Marshall, A. G.; Mcknight, D. M. Characterization of IHSS Pony Lake fulvic acid dissolved organic matter by electrospray ionization Fourier transform ion cyclotron resonance mass spectrometry and fluorescence spectroscopy. *Org. Geochem.* **2013**, *65*, 19−28.

(7) Brezonik, P. L.; Bloom, P. R.; Sleighter, R. L.; Cory, R. M.; Khwaja, A. R.; Hatcher, P. G. Chemical differences of aquatic humic substances extracted by XAD-8 and DEAE-cellulose. *J. Environ. Chem. Eng.* **2015**, *3*, 2982−1994.

(8) Seidel, M.; Beck, M.; Riedel, T.; Waska, H.; Suryaputra, I. G. N. A.; Schnetger, B.; Niggemann, J.; Simon, M.; Dittmar, T. Biogeochemistry of dissolved organic matter in an anoxic intertidal creek bank. *Geochim. Cosmochim. Acta* **2014**, *140*, 418−434.

(9) Dubinenkov, I.; Flerus, R.; Schmitt-Kopplin, P.; Kattner, G.; Koch, B. P. Origin-specific molecular signatures of dissolved organic matter in the Lena Delta. *Biogeochemistry* **2015**, *123*, 1−14.

(10) He, C.; Jiang, B.; Shi, Q.; Hsu, C. S. Comment on "Laser Desorption/Ionization Coupled to FTICR Mass Spectrometry for Studies of Natural Organic Matter". *Anal. Chem.* **2018**, *90*, 5965−5967.

(11) Pan, Q.; Zhuo, X.; He, C.; Zhang, Y.; Shi, Q. Validation and Evaluation of High-Resolution Orbitrap Mass Spectrometry on Molecular Characterization of Dissolved Organic Matter. *ACS Omega* **2020**, *5*, 5372−5379.

(12) Shi, Q.; Hou, D.; Chung, K. H.; Xu, C.; Zhao, S.; Zhang, Y. Characterization of Heteroatom Compounds in a Crude Oil and Its Saturates, Aromatics, Resins, and Asphaltenes (SARA) and Non-basic Nitrogen Fractions Analyzed by Negative-Ion Electrospray Ionization Fourier Transform Ion Cyclotron Resonance Mass Spectrometry. *Energy Fuels* **2010**, *24*, 2545−2553.

(13) Smith, D. F.; Podgorski, D. C.; Rodgers, R. P.; Blakney, G. T.; Hendrickson, C. L. 21 Tesla FT-ICR Mass Spectrometer for Ultrahigh-Resolution Analysis of Complex Organic Mixtures. *Anal. Chem.* **2018**, *90*, 2041−2047.

(14) Mopper, K.; Stubbins, A.; Ritchie, J. D.; Bialk, H. M.; Hatcher, P. G. Advanced Instrumental Approaches for Characterization of Marine Dissolved Organic Matter: Extraction Techniques, Mass Spectrometry, and Nuclear Magnetic Resonance Spectroscopy. *Chem. Rev.* **2007**, *107*, 419−442.

(15) Wagner, S.; Fair, J. H.; Matt, S.; Hosen, J.; Raymond, P.; Saiers, J.; Shanley, J.; Dittmar, T.; Stubbins, A. Molecular hysteresis: Hydrologically-driven changes in riverine dissolved organic matter chemistry during a storm event. *J. Geophys. Res.: Biogeosci.* **2019**, *124*, 759−774.

(16) Dvorski, S. E. M.; Gonsior, M.; Hertkorn, N.; Uhl, J.; Mueller, H.; Griebler, C.; Schmitt-Kopplin, P. Geochemistry of Dissolved Organic Matter in a Spatially Highly Resolved Groundwater Petroleum Hydrocarbon Plume Cross-Section. *Environ. Sci. Technol.* **2016**, *50*, 5536−5546.

(17) Geng, C.; Cao, N.; Xu, W.; He, C.; Yuan, Z.; Liu, J.; Shi, Q.; Xu, C.; Liu, S.; Zhao, H. Molecular characterization of organics removed by a covalently bound inorganic−organic hybrid coagulant for advanced treatment of municipal sewage. *Environ. Sci. Technol.* **2018**, *52*, 12642−12648.

(18) Li, Y.; Fang, Z.; He, C.; Zhang, Y.; Xu, C.; Chung, K. H.; Shi, Q. Molecular characterization and transformation of dissolved organic matter in refinery wastewater from water treatment processes: characterization by fourier transform ion cyclotron resonance mass spectrometry. *Energy Fuels* **2015**, *29*, 6956−6963.

(19) Zherebker, A.; Shirshin, E.; Rubekina, A.; Kharybin, O.; Kononikhin, A.; Kulikova, N. A.; Zaitsev, K. V.; Roznyatovsky, V. A.; Grishin, Y. K.; Perminova, I. V.; Nikolaev, E. N. Optical Properties of Soil Dissolved Organic Matter Are Related to Acidic Functions of Its Components as Revealed by Fractionation, Selective Deuteromethylation, and Ultrahigh Resolution Mass Spectrometry. *Environ. Sci. Technol.* **2020**, *54*, 2667−2677.

(20) Xu, C.; Zhang, S.; Kaplan, D. I.; Ho, Y.-F.; Schwehr, K. A.; Roberts, K. A.; Chen, H.; DiDonato, N.; Athon, M.; Hatcher, P. G.; Santschi, P. H. Evidence for Hydroxamate Siderophores and Other N-Containing Organic Compounds Controlling (239,240)Pu Immobilization and Remobilization in a Wetland Sediment. *Environ. Sci. Technol.* **2015**, *49*, 11458−11467.

(21) Jiang, B.; Liang, Y.; Xu, C.; Zhang, J.; Hu, M.; Shi, Q. Polycyclic Aromatic Hydrocarbons (PAHs) in Ambient Aerosols from Beijing: Characterization of Low Volatile PAHs by Positive-Ion Atmospheric Pressure Photoionization (APPI) Coupled with Fourier Transform Ion Cyclotron Resonance. *Environ. Sci. Technol.* **2014**, *48*, 4716−4723.

(22) Fievre, A.; Solouki, T.; Marshall, A. G.; Cooper, W. T. High-resolution Fourier transform ion cyclotron resonance mass spectrometry of humic and fulvic acids by laser desorption/ionization and electrospray ionization. *Energy Fuels* **1997**, *11*, 554−560.

(23) Kim, S.; Simpson, A. J.; Kujawinski, E. B.; Freitas, M. A.; Hatcher, P. G. High resolution electrospray ionization mass spectrometry and 2D solution NMR for the analysis of DOM extracted by C-18 solid phase disk. *Org. Geochem.* **2003**, *34*, 1325−1335.

(24) Dittmar, T.; Koch, B.; Hertkorn, N.; Kattner, G. A simple and efficient method for the solid-phase extraction of dissolved organic matter (SPE-DOM) from seawater. *Limnol. Oceanogr.: Methods* **2008**, *6*, 230−235.

(25) Sleighter, R. L.; Hatcher, P. G. The application of electrospray ionization coupled to ultrahigh resolution mass spectrometry for the molecular characterization of natural organic matter. *J. Mass Spectrom.* **2007**, *42*, 559−574.

(26) Hockaday, W. C.; Purcell, J. M.; Marshall, A. G.; Baldock, J. A.; Hatcher, P. G. Electrospray and photoionization mass spectrometry for the characterization of organic matter in natural waters: a qualitative assessment. *Limnol. Oceanogr.: Methods* **2009**, *7*, 81−95.

(27) Rivas-Ubach, A.; Liu, Y.; Bianchi, T. S.; Tolic, N.; Jansson, C.; Pasa-Tolic, L. Moving beyond the van Krevelen Diagram: A New Stoichiometric Approach for Compound Classification in Organisms. *Anal. Chem.* **2018**, *90*, 6152−6160.

(28) Koch, B. P.; Dittmar, T. From mass to structure: an aromaticity index for high-resolution mass data of natural organic matter. *Rapid Commun. Mass Spectrom.* **2006**, *20*, 926−932.

(29) Sleighter, R. L.; McKee, G. A.; Hatcher, P. G. Direct Fourier transform mass spectral analysis of natural waters with low dissolved organic matter. *Org. Geochem.* **2009**, *40*, 119−125.

(30) Medeiros, P. M.; Seidel, M.; Powers, L. C.; Dittmar, T.; Hansell, D. A.; Miller, W. L. Dissolved organic matter composition and photochemical transformations in the northern North Pacific Ocean. *Geophys. Res. Lett.* **2015**, *42*, 863−870.

(31) Šantl-Temkiv, T.; Finster, K.; Dittmar, T.; Hansen, B. M.; Thyrhaug, R.; Nielsen, N. W.; Karlson, U. G. Hailstones: A Window into the Microbial and Chemical Inventory of a Storm Cloud. *PLoS One* **2013**, *8*, No. e53550.

(32) D'Andrilli, J.; Cooper, W. T.; Foreman, C. M.; Marshall, A. G. An ultrahigh-resolution mass spectrometry index to estimate natural organic matter lability. *Rapid Commun. Mass Spectrom.* **2015**, *29*, 2385−2401.

(33) Medeiros, P. M.; Seidel, M.; Niggemann, J.; Spencer, R. G. M.; Hernes, P. J.; Yager, P. L.; Miller, W. L.; Dittmar, T.; Hansell, D. A. A novel molecular approach for tracing terrigenous dissolved organic matter into the deep ocean. *Global Biogeochem. Cycles* **2016**, *30*, 689−699.

(34) Hertkorn, N.; Benner, R.; Frommberger, M.; Schmitt-Kopplin, P.; Witt, M.; Kaiser, K.; Kettrup, A.; Hedges, J. I. Characterization of a major refractory component of marine dissolved organic matter. *Geochim. Cosmochim. Acta* **2006**, *70*, 2990−3010.

(35) Flerus, R.; Lechtenfeld, O. J.; Koch, B. P.; Mccallister, S. L.; Schmittkopplin, P.; Benner, R.; Kaiser, K.; Kattner, G. A molecular perspective on the ageing of marine dissolved organic matter. *Biogeosciences* **2012**, *9*, 1935−1955.

(36) Lechtenfeld, O. J.; Kattner, G.; Flerus, R.; McCallister, S. L.; Schmitt-Kopplin, P.; Koch, B. P. Molecular transformation and degradation of refractory dissolved organic matter in the Atlantic and Southern Ocean. *Geochim. Cosmochim. Acta* **2014**, *126*, 321−337.

(37) Witt, M.; Fuchser, J.; Koch, B. P. Fragmentation Studies of Fulvic Acids Using Collision Induced Dissociation Fourier Transform Ion Cyclotron Resonance Mass Spectrometry. *Anal. Chem.* **2009**, *81*, 2688−2694.

(38) Zark, M.; Christoffers, J.; Dittmar, T. Molecular properties of deep-sea dissolved organic matter are predictable by the central limit theorem: Evidence from tandem FT-ICR-MS. *Mar. Chem.* **2017**, *191*, 9−15.

(39) Koch, B. P.; Witt, M.; Engbrodt, R.; Dittmar, T.; Kattner, G. Molecular formulae of marine and terrigenous dissolved organic matter detected by electrospray ionization Fourier transform ion cyclotron resonance mass spectrometry. *Geochim. Cosmochim. Acta* **2005**, *69*, 3299−3308.

(40) Ohno, T.; He, Z.; Sleighter, R. L.; Honeycutt, C. W.; Hatcher, P. G. Ultrahigh Resolution Mass Spectrometry and Indicator Species Analysis to Identify Marker Components of Soil- and Plant Biomass-Derived Organic Matter Fractions. *Environ. Sci. Technol.* **2010**, *44*, 8594−8600.

(41) Kujawinski, E. B.; Longnecker, K.; Blough, N. V.; Del Vecchio, R.; Finlay, L.; Kitner, J. B.; Giovannoni, S. J. Identification of possible source markers in marine dissolved organic matter using ultrahigh resolution mass spectrometry. *Geochim. Cosmochim. Acta* **2009**, *73*, 4384−4399.

(42) D'Andrilli, J.; Junker, J. R.; Smith, H. J.; Scholl, E. A.; Foreman, C. M. DOM composition alters ecosystem function during microbial processing of isolated sources. *Biogeochemistry* **2019**, *142*, 281−298.

(43) Wu, X.; Wu, L.; Liu, Y.; Zhang, P.; Li, Q.; Zhou, J.; Hess, N. J.; Hazen, T. C.; Yang, W.; Chakraborty, R. Microbial Interactions With Dissolved Organic Matter Drive Carbon Dynamics and Community Succession. *Front. Microbiol.* **2018**, *9*, 1234.

(44) Vorobev, A.; Sharma, S.; Yu, M.; Lee, J.; Washington, B. J.; Whitman, W. B.; Ballantyne, F.; Medeiros, P. M.; Moran, M. A. Identifying labile DOM components in a coastal ocean through depleted bacterial transcripts and chemical signals. *Environ. Microbiol.* **2018**, *20*, 3012−3030.

(45) Ly, L. V.; Hur, J. Further insight into the roles of the chemical composition of dissolved organic matter (DOM) on ultrafiltration membranes as revealed by multiple advanced DOM characterization tools. *Chemosphere* **2018**, *201*, 168−177.

(46) Powers, L. C.; Luek, J. L.; Schmitt-Kopplin, P.; Campbell, B. J.; Magen, C.; Cooper, L. W.; Gonsior, M. Seasonal changes in dissolved organic matter composition in Delaware Bay, USA in March and August 2014. *Org. Geochem.* **2018**, *122*, 87−97.

(47) Schmidt, F.; Koch, B. P.; Goldhammer, T.; Elvert, M.; Witt, M.; Lin, Y.-S.; Wendt, J.; Zabel, M.; Heuer, V. B.; Hinrichs, K.-U. Unraveling signatures of biogeochemical processes and the depositional setting in the molecular composition of pore water DOM across different marine environments. *Geochim. Cosmochim. Acta* **2017**, *207*, 57−80.

(48) Blackburn, J. W. T.; Kew, W.; Graham, M. C.; Uhrin, D. Laser Desorption/Ionization Coupled to FTICR Mass Spectrometry for Studies of Natural Organic Matter. *Anal. Chem.* **2017**, *89*, 4382−4386.

(49) Enke, C. G. A Predictive Model for Matrix and Analyte Effects in Electrospray Ionization of Singly-Charged Ionic Analytes. *Anal. Chem.* **1997**, *69*, 4885−4893.

(50) Limbach, P. A.; Grosshans, P. B.; Marshall, A. G. Experimental determination of the number of trapped ions, detection limit, and dynamic range in Fourier transform ion cyclotron resonance mass spectrometry. *Anal. Chem.* **1993**, *65*, 135−140.

(51) Marshall, A. G.; Hendrickson, C. L.; Jackson, G. S. Fourier transform ion cyclotron resonance mass spectrometry: a primer. *Mass Spectrom. Rev.* **1998**, *17*, 1−35.

(52) Marshall, A. G.; Chen, T. 40 years of Fourier transform ion cyclotron resonance mass spectrometry. *Int. J. Mass Spectrom.* **2015**, *377*, 410−420.

(53) Kido Soule, M. C.; Longnecker, K.; Giovannoni, S. J.; Kujawinski, E. B. Impact of instrument and experiment parameters on reproducibility of ultrahigh resolution ESI FT-ICR mass spectra of natural organic matter. *Org. Geochem.* **2010**, *41*, 725−733.

(54) Sleighter, R. L.; Chen, H.; Wozniak, A. S.; Willoughby, A. S.; Caricasole, P.; Hatcher, P. G. Establishing a measure of reproducibility of ultrahigh-resolution mass spectra for complex mixtures of natural organic matter. *Anal. Chem.* **2012**, *84*, 9184−9191.

(55) Kujawinski, E. B.; Behn, M. D. Automated analysis of electrospray ionization fourier transform ion cyclotron resonance mass spectra of natural organic matter. *Anal. Chem.* **2006**, *78*, 4363−4373.